Processing and characterisation of standard and doped alite-belite-ye'elimite ecocement pastes and mortars

Jesus D. Zea-Garcia[1], Angeles G. De la Torre[1], Miguel A.G. Aranda[1,2], Isabel Santacruz[1]*

[a] Departamento de Química Inorgánica, Cristalografía y Mineralogía, Universidad de Málaga, Málaga, 29071, Spain.

[b] ALBA Synchroton, Carrer de la Lum, 2-26, Cerdanyola, 08290, Barcelona-Spain.

* email: isantacruz@uma.es. Phone: +34.952131878. Fax: +34.952131870

KEYWORDS: Alite-belite-ye'elimite ecocements; Processing; Rheology; X-ray diffraction; Compressive Strength.

ABSTRACT*:* Here, we report the processing optimisation of two laboratory-prepared alite-belite-ye'elimite ecocements (standard and doped) that release to the atmosphere ~13% less CO_2 than Portland Cement during fabrication. The processing was optimised through rheological measurements, where homogeneous pastes and mortars were finally prepared through the study and optimisation of both the superplasticizer content and the water-to-cement ratio. Both parameters were correlated with the phase assembly of selected pastes and compressive strength of the corresponding mortars. After optimisation, mortars with high compressive strengths (~72 and ~77 MPa for the standard mortar, and ~41 and ~75 MPa for the doped one, at 7 and 28 days, respectively) were prepared. The important increase in compressive strength from 7 to 28 days of

the optimised mortar prepared from the doped ecocement is due to its composition (the higher content of belite jointly with the reaction of its active polymorph (α'_H-belite)).

1. Introduction

During the fabrication of Portland Cement (PC), large amounts of CO_2 are released to the atmosphere (~0.98 tons of CO_2 per ton of PC) [1], which makes the cement industry responsible of ~6% of the anthropogenic CO_2 emissions [2]. These emissions are mainly due to the decarbonation of calcite to achieve the desired composition after clinkering. PC is mainly composed of ~65 wt% of alite (Ca_3SiO_5 or $3CaO{\cdot}SiO_2$) and ~15 wt% of belite (Ca_2SiO_4 or $2CaO{\cdot}SiO_2$), which are high calcite-demanding phases, mainly alite. There is a phase named ye'elimite ($Ca_4Al_6SO_{16}$ or $4CaO{\cdot}3Al_2O_3{\cdot}SO_3$) that is not present in PC, which contributes with 0.22 tons of CO_2 per ton of phase produced while alite contributes with 0.58 tons/ton of phase (~38% less emissions). Thus, ye'elimite rich-cements may be a good alternative to PC, if they can achieve similar performance, achieving savings around 25-30% of CO_2 emissions depending on the composition [3]. Alite-Belite-Ye'elimite (ABY) cement, where alite has been partially substituted by ye'elimite, may be a good alternative [4,5,6,7,8]. These cements can be considered as ecocements due to the lower amount of CO_2 that it is released during fabrication, where the reduction achieved depends on the composition. It is known that belite can present polymorphism, where the polymorph found in PC is β-belite; however, α-forms of belite or modified β-belite promote higher mechanical strengths than the beta form at early ages [9]. This fact is interesting in order to achieve high mechanical properties.

To achieve good performance, it is essential to optimise the processing of cement pastes/mortars to improve their workability and obtain homogeneous and dense materials. This is reached through the preparation of well dispersed cement pastes [10,11]. In addition, low water contents, within certain limits, are usually related with improved mechanical properties [12,13]. The use of superplasticisers is a common practice in the building industry since it helps the dispersion of

the cement particles, reduces viscosity and allows the preparation of lower water-to-cement (w/c) ratios. The superplasticiser is adsorbed onto the surface of cement particles causing the repulsion of the particles through electrostatic, steric or electrosteric repulsions [14,15,16,17,18]. The repulsion will depend [10] on the superplasticiser (type and amount), the composition of the cement powder, particle size distribution and hence specific surface area, and so on. Specific additives (retarders and/or specific superplasticisers, such as polycarboxylate-based superplasticisers) can slow down the reactions which may be beneficial to improve the workability in particular systems [13,19]. The addition of the right amount of chemical admixture is key to improve the dispersion, reduce the viscosity and control the setting time, to finally improve the homogeneity and performance of the corresponding cements and mortars. Because of that, in this work, the superplasticiser content and the water-to-cement ratio have been optimised.

Furthermore, the hydration reactions need to be fully understood and the mechanical properties have to be under control, since they are usually related to both processing and phase assembly. The hydration procedure of cements consists in three steps: dissolution of the anhydrous phases, saturation of the liquid medium, and formation of new phases, with the corresponding water consumption. Thus, equations 1-3 show the reactions of alite, belite and ye'elimite with water, respectively. The latter also reacts with the sulphate source in water.

$$Ca_3SiO_5 + 5.2H_2O \rightarrow (CaO)_{1.8}SiO_2\,(H_2O)_4 + 1.2\,Ca(OH)_2 \qquad \text{Eq. 1}$$

$$Ca_2SiO_4 + 4.2H_2O \rightarrow (CaO)_{1.8}SiO_2\,(H_2O)_4 + 0.2\,Ca(OH)_2 \qquad \text{Eq. 2}$$

$$Ca_4Al_6O_{12}SO_4 + 2\,CaSO_4{\cdot}xH_2O + (38\text{-}2x)\,H_2O \rightarrow Ca_6Al_2(OH)_{12}(SO_4)_3{\cdot}26H_2O + 4\,Al(OH)_3$$

(x=0, 0.5, 2, for anhydrite, bassanite and gypsum, respectively) Eq. 3

Alite and belite react with water producing heterogeneous nanocrystalline C-S-H gel ($(CaO)_{1.8}SiO_2$ $(H_2O)_4$) and crystalline portlandite ($Ca(OH)_2$) [20], where the former provides the cement with high mechanical strengths. Ye'elimite reacts with the sulphate source in presence of water to produce crystalline ettringite ($Ca_6Al_2(OH)_{12}(SO_4)_3 \cdot 26H_2O$) and nanocrystalline gibbsite ($Al(OH)_3$), where the former also produces high mechanical strengths at early ages.

The objective of this work is the preparation of mortars prepared from ecocements that release ~17% less CO_2 than PC during manufacturing but maintains the same performance. For that, two laboratory-prepared cement pastes, standard and doped Alite-Belite-Ye'elimite (ABY and dABY, respectively), were prepared and optimised in terms of superplasticiser and water contents, through rheological measurements. The hydration of the pastes was controlled through laboratory X-ray powder diffraction, and the compressive strength of the corresponding mortars was measured and discussed according to the processing parameters and phase assembly. Finally, the processing parameters resulted to be key to achieve ABY mortars with high mechanical strength values, even higher than those for PC at certain ages.

2. Material and Methods

2.1. Materials.

2.1.1 Clinker preparation.

Here, the final optimised procedure was followed: as raw materials, natural gypsum, natural limestone (both from Financiera y Minera cement factory, Spain), Kaolin (ref. NC-35, Caolines Vimianzo, Spain), iron ore (by-product of the sulphuric acid industry) and natural sand were

used. As mineralizers/activators, CaF_2 (≥99%, Sigma-Aldrich), ZnO (added as $ZnSO_4 \cdot H_2O$, ≥99%, Sigma-Aldrich) and $Na_2B_4O_7 \cdot 10H_2O$ (VWR, Prolabo) were added.

The preparation of two types of Alite-Belite-Ye'elimite clinkers (standard and doped) was reported elsewhere [21]. Here, the final optimised procedure was followed. The standard clinker (ABY) is composed of alite, β-belite and ye'elimite, and was obtained by adding 1 wt% of CaF_2 and 1 wt% of ZnO to the raw mix. To prepare the doped clinker (dABY), 0.6 wt% of B_2O_3 and 0.3 wt% of Na_2O, added as borax, was added to the raw mix, which also contained CaF_2 (1 wt%) and ZnO (1 wt%). This clinker has β and α'_H-belite, alite and ye'elimite.

The raw mixtures were die-pressed (35 g and 55 mm of diameter), clinkered (900°C/30 min and 1300°C/15 min; heating rate of 5°C/min) and quenched using forced air convection in groups of six pellets using a Pt/Rh crucible. This method was repeated various times to obtain ~2 kg of both clinkers (standard and doped). Clinkers were ground in a vibration disc mill up to similar media particle/agglomerate size distribution (similar d_{v50}), and the corresponding Blaine values are 2628 ± 29 and 2399 ± 31 cm²/g, for ABY and dABY, respectively.

2.1.2. Cement paste preparation.

Both clinkers were mixed with 14 wt% of anhydrite to prepare the corresponding cements (being this the stoichiometric amount of calcium sulfate needed to react with ye'elimite/aluminates to yield ettringite). Anhydrite was prepared by heating commercial bassanite (BELITH S.P.R.L., Belgium) at 700°C/1h.

Cement pastes were prepared with deionized water using water-to-cement mass ratios of 0.40, 0.50 and 0.55 following a modified UNE-EN 196-3 standard, where a mechanical stirrer was used and a fixed speed of 800 rpm was selected. The amount of a polycarboxylate-based superplasticiser, SP, (from 0.0 to 1.0 wt% of active matter referred to the cement content)

(Floadis 1623, Adex Polymer S.L., Madrid, Spain) was optimised with pastes prepared at w/c of 0.40. The SP contains 25 wt% of active matter. The water present in the superplasticizer was considered for the overall w/c ratio of the paste. Selected pastes were cast into hermetically closed polytetrafluoroethylene (PTFE) cylinders, and were rotated (16 rpm) during the first 24 h at 20 ± 1ºC. After that, pastes were introduced in water at 20 ± 1ºC for 1, 7, 28 and 56 days. Prior to laboratory X-ray powder diffraction (LXRPD) characterisation, the hydration of the cement pastes was stopped; for that, samples were manually grinded, and washed twice with isopropanol, and once with diethyl ether.

2.1.3. Mortar preparation.

Mortars were prepared according to UNE-EN196-1 at the cement/sand mass ratio of 1/3 and w/c ratios of 0.40 and 0.50. Mortars were prepared with selected amounts of superplasticiser (0.4 and 1.0 wt% referred to cement). For the sake of comparison, PC mortars (CEM1 52.5N) prepared at a w/c ratio of 0.40 with 0.2 wt% (active matter) of the same superplasticiser were also characterised. In all cases, CN EN196-1 standard sand was used. Mortar cubes ($3 \times 3 \times 3$ cm^3) were cast and cured at 20 ± 1°C and 99% relative humidity (RH) for 24 h. The cubes were demoulded and kept in a water bath (20 ± 1°C) for 1, 7, 28, 56 and 180 curing days when the compression strengths were measured.

2.2. Characterisation.

2.2.4. Rheological behaviour of cement pastes.

The effect of the superplasticiser on the rheological behaviour of the cement pastes (w/c=0.40) was studied. A viscometer (Model VT550, Thermo Haake, Karlsruhe, Germany) with a serrated coaxial cylinder sensor, SV2P, provided with a lid to reduce evaporation was used. The water

demand of pastes was also studied through their rheological behaviour, by preparing pastes at different w/c ratios, 0.40, 0.50 and 0.55, with selected amounts of SP (0.0, 0.4 and 1.0 wt%).

Two different measurements were performed: i) flow curves (controlled rate measurements), where ramp times of 6 s were recorded in the shear rate range between 2 and 350 s^{-1}, for a total of 12 ramps. A further decrease of shear rate from 350 to 2 s^{-1} was performed by following the same ramp times. Prior to any rheological measurement, all pastes were pre-sheared for 30 s at 350 s^{-1} and held at 0 s^{-1} for 5 s in the viscometer; flow curves were measured after 5 min since cement and water were mixed. ii) viscosity vs. time measurements, at a fixed shear rate of 5 s^{-1}.

2.2.5. Laboratory X-Ray Powder Diffraction (LXRPD) data collection.

Patterns of the anhydrous cements and selected pastes (1, 7, 28 and 56 days, after arresting hydration) were recorded on a diffractometer (X'Pert MPD PRO, PANalytical) located at Servicios Centrales de Apoyo a la Investigación (SCAI) at University of Malaga (Spain). It contains a Ge (111) primary Johanson monochromator that provides strictly monochromatic CuKα_1 radiation (λ=1.54059Å) and a X'Celerator RTMS (Real Time Multiple Strip) detector, working in scanning mode with maximum length. The X-ray tube worked at 45 kV and 40 mA. Patterns were collected from 5º to 70° (2θ) during ~2 h using a spinning sample-holder (16 rpm) to enhance particle statistics.

2.2.6. LXRPD data analysis

The powder patterns were analysed by Rietveld method using the GSAS [22] software package, by using a pseudo-Voigt peak shape function with the asymmetry correction included [23,24], to obtain Rietveld Quantitative Phase Analysis (RQPA). The refined overall parameters were: background coefficients, phase scale factors, unit cell parameters, zero-shift error, peak shape parameters and preferred orientation coefficient, if needed. The crystal structure descriptions

used for all phases are given elsewhere [21]. The amorphous and crystalline non-quantified content (ACn) of all pastes was calculated using an external standard method (G-factor approach) [25].

2.2.7. Thermal analysis.

A SDT-Q600 analyser (TA instruments, New Castle, DE) was used to perform thermogravimetric (TGA) analyses of the pastes already studied through LXRPD (after stopping hydration). Samples were heated from room temperature (RT) to 1000°C (at 10°C/min) in open platinum crucibles under air flow. The weighed loss from RT to 600°C was assigned as chemically bounded water and the weighed loss from 600 to 1000°C was considered as CO_2. The free water content (FW), in wt%, was calculated for each cement paste using Equations 4 and 5.

$$BW = (BW_{ATD} \times CM) / (100 - BW_{ATD}) \quad \text{Eq. 4}$$

$$FW = TW - BW \quad \text{Eq. 5}$$

Where BW corresponds to chemically bound water content, TW is the total water content, BW_{ATD} is the loss of mass measured up to 600ºC from DTA-TGA curves (which is considered bound water in a paste after stopping hydration), and CM is the cement content (all the numbers in weight percentage).

2.2.8. Microstructural characterisation: Scanning Electron Microscopy (SEM), Laser diffraction and BET.

The fracture surfaces of both die-pressed clinker pellets were observed using a Jeol JSM-840 (Japan) scanning electron microscope (SEM) to characterise the primary particles (phases). The size and shape of the aggregates of both clinkers after milling were also observed by SEM.

The aggregate size distribution of both milled clinker powders was measured through laser diffraction (MastersizerS, Malvern) provided with a wet sample cell (using ethanol as organic solvent).

The specific surface area of both clinker powders was carried out by BET method (Brunauer–Emmett–Teller) using nitrogen, with an automatic Micromeritics Asap 2020 equipment. The Blaine data (air permeability method) of the clinkers were also measured.

2.2.9. Compressive strengths

The compressive strength of the cubic mortars ($3 \times 3 \times 3$ cm^3) was measured in a press (Model Autotest 200/10 W, Ibertest, Spain) at selected curing ages. Three cubic mortars were tested at every studied hydration ages which allows obtaining the average value and its associated standard deviation (UNE-EN196-1). A correction factor was applied to the measured values allowing direct comparison to those obtained with standard prisms ($4 \times 4 \times 16$ cm^3).

3. Results and Discussion

Figures 1.a and 1.b show SEM micrographs of the fracture surfaces of both standard and doped die-pressed clinker pellets, respectively. Main phases are labelled in the micrographs, as they were identified due to their morphology [26]. Belite particles show their characteristic round shapes, and ye'elimite particles show hexagonal ones. As it was already reported [26], the presence of ZnO promoted the formation of elongated alite particles. In addition, belite particles in the doped clinker are much larger than in the standard one. This is related to the presence of borax in the doped clinker, which decreases the formation temperature of the liquid phase [27] and favours the growth of the particles.

The clinker pellets were milled to similar media particle/aggregate sizes (d_{v50} of 7.9 and 8.9 μm for standard and doped clinkers, respectively). Values of d_{v10} were also similar, but the values of d_{v90} were 38.8 and 19.4 μm for standard and doped clinkers, respectively. Figures 1.c y 1.d correspond to the SEM micrographs of both milled powders, ABY and dABY respectively. The surface area values obtained by BET for ABY and dABY clinkers are 1.56 and 1.19 m^2/g, respectively. In both cases, the tendency is in agreement with the $d_{v,50}$ values (low $d_{v,50}$ and high surface area values). The BET method gives higher data than the Blaine methodology because the former includes internal surfaces present in microcracks or in pores open at only one end [28].

Once both powders were characterised, anhydrous cements were prepared. Table 1 shows the phase assemblage of both anhydrous cements, including the ACn content. The standard cement (ABY) is mainly formed by alite, β-belite and ye'elimite, and the doped cement (dABY) is chiefly formed by β and α'_H-belite, alite and ye'elimite. Although in the latter the amount of belite is higher than the content of alite, the same terminology has been used in both cases.

The optimized SP content for pastes with w/c of 0.4 was determined by rheological studies. Figure S1, deposited as supplementary material, shows the flow curves of ABY and dABY pastes prepared at a w/c ratio of 0.40 and different SP contents. The flow curves of the pastes prepared at w/c of 0.50 with 0.4 wt% SP are also shown for the sake of comparison; the viscosity of those pastes is lower at any shear rate at very early ages, as expected, due to the higher water content. Figures 2.a and 2.b show the deflocculation curves of both families (w/c=0.40), at 50 s^{-1} and 200 s^{-1}, respectively. Values were taken from the down-curves of Figure S1 deposited as supplementary material. All of them show a shear thinning behaviour, where all the viscosity values at 200 s^{-1} are lower than those measured at 50 s^{-1}. In both families, the shear stress and

consequently the viscosity decrease by increasing the SP content, down to a minimum (saturation point). In both families, a minimum viscosity values, and hence good dispersion, are achieved for 0.4 wt% of SP, Figure 2.a and 2.b and S1; for dABY paste this happens only at shear rate values lower than 150 s^{-1}, since at higher shear rates, the minimum viscosity is achieved when 1.0 wt% of SP is added (Figures 2.b and S1).

At very early hydration times, both families show similar tendencies, Figure 2.a, and their viscosity values at 50 s^{-1} are quite similar (although there are some exceptions). At high shear rates, e.g. 200 s^{-1}, the viscosity values of dABY pastes are slightly higher than those for ABY pastes. When SP is not added, the viscosity of the dABY paste is higher than that for the ABY paste at both shear rates. Since both powders show a similar media aggregate size (slightly larger for dABY), and the primary particle size in dABY is also larger, this may be attributed to the percentage of large particles of ABY that were not milled properly (ABY shows higher d_{v90} than dABY) but mainly to high speed of hydration of mayenite ($C_{12}A_7$) which is only present in dABY [29], Table 1.

It is worth to highlight that the dABY paste with 1 wt% SP, Figures 2.b, and S1, shows the lowest viscosity values at shear rates higher than 50 s^{-1}. This fact may be related with the retarder effect of the SP, which will be thoroughly studied below. Table 2 shows the value of the thixotropic cycle of all the studied pastes, which is related with the effect of time and SP content added to the pastes. In general, the lower values were found when 0.4 and 1.0 wt% SP were added. Because of that, and their low viscosity values (Figure 2 and S1), pastes with 0.4 and 1.0 wt% of SP were deeper studied and compared with the pastes without SP.

The water demand of both systems prepared with the selected SP contents (0.0, 0.4 and 1.0 wt%) was also studied. Figures 2.c and 2.d show the viscosity of the pastes vs. w/c ratio for ABY

and dABY pastes with the selected amounts of SP. All these values were taken from the down-curves of the flow curves at 50 s^{-1} (solid lines in Figures 2.c and 2.d) and at 200 s^{-1} (dashed lines in Figures 2.c and 2.d). As expected, the viscosity decreased by increasing the water content. The diminishing in viscosity with increasing amounts of water is more pronounced for systems without SP, due to the stronger structure formed between particles, higher particle interaction, which hinders the flow. ABY pastes prepared with 1.0 wt% SP show slightly lower viscosity values than the equivalent pastes prepared with 0.4 wt% SP with w/c>0.40 (Figures 2.c and 2.d). When dABY pastes are prepared at a low w/c, e.g. w/c=0.40, they need 1.0 wt% SP to achieve the lowest viscosity values (at 200 s^{-1}), but it does not happen when higher water contents are used (w/c=0.50 and 0.55), where pastes with 0.4 wt% SP shows the lowest values (Figures 2.c and 2.d), independently of the shear rate. This may be related with a quick increasing in viscosity with time of the dABY paste at w/c=0.40, and the need of the retardation. To further study this behaviour, the evolution with time of these pastes was characterised.

Figures 3.a and 3.b show the evolution of the viscosity with time of ABY and dABY cement pastes, respectively, prepared with 0.0, 0.4 and 1.0 wt% SP and w/c ratios of 0.40 and 0.50. Pastes were measured at 5 s^{-1} in order to obtain accurate values without destroying the structure (or minimum destruction). In all cases, the viscosity increases with time, as expected. At the initial time, the tendency of the viscosity of ABY pastes, at 5 s^{-1}, Figure 3.a, is the same than that found for 50 and 200 s^{-1} (Figures 2.c and 2.d). ABY pastes with w/c=0.50 shows lower viscosity values, at any time, than the corresponding pastes at w/c=0.40 for the same SP content. In addition, by increasing the SP content, in all cases, a retardation of the rise in viscosity is observed, due to the retarder effect of the polycarboxylate, in agreement with previous studies [19]. This is observed when the ABY paste prepared with w/c=0.40 and 1.0 wt% SP is compared

with the ABY paste with w/c=0.50 and 0.40 wt% SP. Here, although the initial viscosity of the latter is lower, after 14 min of hydration, the rise in viscosity of the paste with the higher amount of SP is much lower. In the case of the dABY family, at 5 s^{-1}, Figure 3.b, the viscosity of pastes prepared with 1.0 wt% SP (w/c=0.40 or 0.50) increases at a slower pace than those prepared with 0.4 wt% SP, where the rise in viscosity is lower for the paste prepared at w/c=0.50, as it happened for ABY pastes. When the evolution of viscosity of the dABY paste prepared with w/c=0.40 and 0.4 wt% SP is compared with that prepared at the same w/c but with 1.0 wt% SP, it is observed that, although at the beginning the paste with 0.4 wt% SP shows lower viscosity, after 12 min of hydration, the increase in viscosity of the paste with 1.0 wt% SP takes place at a slower rate due to the retarder effect of the superplasticiser. This study is important because the control of the evolution of the viscosity during the first minutes of hydration is essential to assure a good initial dispersion but also to guarantee that the viscosity is not increasing dramatically during the mortar preparation. It will allow the preparation of flawless/homogeneous mortars. This is more important for dABY pastes since their increase in viscosity with time is quicker than for ABY ones due to mainly the higher dissolution/reactivity degree of mayenite [29]. All this will have effects on the homogeneity of the systems, and thus on the mechanical properties of the corresponding mortars.

Figure 4 shows the compressive strength values of ABY and dABY mortars prepared with 0.4 and 1.0 wt% of SP at w/c=0.40, and mortars prepared with 0.4 wt% SP at w/c=0.50 at different curing ages. It was not possible to prepare mortars without SP due to their high viscosity.

On the one hand, within the ABY family, the highest values of compressive strength are achieved when they are prepared at w/c=0.40 with 1.0 wt% SP at any hydration time. ABY mortars prepared at w/c=0.50 with 0.4 wt% SP contained more water than the previous ones, and

also suffer a quicker increase in viscosity (Figure 3.a), so they show lower compressive strengths. Although ABY mortars prepared with 0.4 wt% SP and w/c=0.40 could have shown high mechanical strength values, the viscosity of these mortars increased too high with time to prepare flawless samples; consequently, heterogeneous cubes with cracks and porosity were prepared, see insets of Figure 4. However, when 1.0 wt% SP was used in the preparation of ABY mortars with w/c=0.40, they showed very high compressive strengths, mainly due to the lower initial viscosity of the mortar and the retarder effect of the SP, which allowed to have enough time to prepare homogeneous samples (see insets of Figure 4), with the consequent increase in compressive strengths at any age (e.g. 77±2, 86.9±0.3 and 98±3 MPa at 28, 56 and 180 hydration days).

On the other hand, dABY mortars prepared at w/c=0.40, with 0.4 or 1.0 wt% SP, showed lower compressive strength values than mortars prepared at w/c=0.50 with 0.4 wt% SP at any hydration time. As it happened for ABY mortars, those prepared with 0.4 wt% SP at w/c=0.40 showed very high viscosity during the mortar preparation which made impossible to properly homogenise the specimens; consequently, heterogeneous cubes, with cracks and porosity were obtained, see insets of Figure 4. This fact is more dramatic for dABY than for ABY mortars due to its higher viscosity, and because of that, mechanical strengths are lower. dABY mortars with w/c=0.40 and 1.0 wt% SP also showed low mechanical strengths values due to the heterogeneity and defects of the mortars (inset of Figure 4). However, when a higher water content, w/c=0.50, and the right amount of SP, 0.4 wt% were added, homogeneous dABY specimens were prepared (they show lower initial viscosity than the paste with w/c=0.4 and 1.0 wt% SP), see insets of Fig. 4, with the consequent increase in strength. ABY and dABY mortars were not prepared at w/c=0.50 with 1.0 wt% SP to avoid too much retardation.

Although the control of the initial viscosity and its evolution with time of dABY system (Figure 3.b) has made possible the preparation of homogeneous mortars that show high mechanical strengths (dABY_0.50w/c_0.4wt%SP), they are lower than the optimised ABY mortars at certain ages (< 28 days), even after optimisation. However, it is worth to highlight the rise in compressive strength from 7 to 28 days in the optimised dABY mortars (w/c=0.50, 0.4 wt% SP), from 41±1 to 75±2 MPa. This is related with the presence of the more active polymorph of belite, α'_H-belite phase (Table 1) [21]. Optimised dABY mortars show quite high compressive strengths, mainly from 28 curing days (e.g. 75±2, 82±2 and 83±6 MPa at 28, 56 and 180 hydration days); these values at 28 and 56 days are very similar to those obtained for ABY mortars.

The mechanical strength values of the optimised ABY mortars (w/c=0.40 and 1.0 wt% SP) are higher than those obtained for PC (PC_0.40w/c_0.2wt%SP) at early ages (1 and 7 days) or equivalent to them (56, 180 days), see Figure 4.

With the aim of understanding the hydration of these ABY and dABY pastes and also correlating mineralogical composition with mechanical strengths for homogeneous specimens, LXRPD was performed on four selected pastes (ABY_0.40wc_1.0SP, ABY_0.50wc_0.4SP, dABY_0.40wc_1.0SP, and dABY_0.50wc_0.4SP) at different ages. The phase assemblage of those optimised selected pastes, including amorphous content and free water, at 0, 1, 7, 28 and 56 days is shown in Figure 5. Tables S1 to S5 (provided as supplementary information) give the full phase assemblage of all pastes in order to detailed the minor anhydrous and hydrated phases that have been merged to one value in Figure 5. Rietveld low disagreement factors were achieved for all pastes. Figures S2.a and S2.b, Supplementary Information, show the Rietveld plots of selected ABY (ABY_0.40wc_1.0SP) and dABY pastes (dABY_0.50wc_0.4SP) at 56 hydration

days, as representative examples, where the most important phases are labelled. These plots have been selected because they correspond to the mortars with the highest mechanical strengths.

The evolution with time of ettringite (one of the most important hydration phases of this type of cements), ACn and free water contents of the four selected pastes is shown in Figures 6.a, 6.b and 6.c, respectively, for a better visualisation. In general, high ettringite, high ACn, and low free water (as indicative of the evolution of the hydration) contents are related to high mechanical properties. During hydration, the ettringite content of all pastes at ages higher than 7 days decreases due to its decomposition likely due to the silicate-rich environment and the increase in pH [30].

The evolution of these three parameters with time within the four samples, Figure 6, cannot justify the mechanical properties of the corresponding mortars. Thus, this confirms that the optimisation of the processing is the most important parameter to improve the properties of these materials through the preparation of homogeneous specimens. Nevertheless, it is worth to highlight that, from 7 to 28 days of hydration, dABY mortars have increased their ACn content (Figure 6.b) and also their compressive strength (Figure 5) have increased much more than the other samples. This is due to the high belite content, that reacts at high ages, jointly with the fact that it contains α'_H-belite, which is a more reactive polymorph (and the homogenisation).

Table 3 gives the degree of reaction of the main phases at all the studied ages for the four selected pastes calculated from the data given in Tables S1 to S5. Alite is very reactive in all the cements pastes, while β-belite is more reactive in doped cement. The higher reactivity of α'_H-belite than that of β-belite is also proved in these systems.

4. Conclusions

Alite-Belite-Ye'elimite (ABY) and doped-Alite-Belite-Ye'elimite (dABY) cements were prepared in the laboratory. The former is composed of alite, β-belite and ye'elimite, and the latter contained β-belite, α'_H-belite, alite and ye'elimite. The amounts of alite and ye'elimite in dABY were lower than in ABY cements, while the belite amount was higher.

The optimisation of both cement pastes (in terms of superplasticiser and water content) through their rheological behaviour allowed the preparation of homogeneous pastes and mortars (ABY prepared at w/c=0.40 with 1.0 wt% SP and dABY prepared at w/c=0.50 with 0.4 wt% SP). The control of the initial viscosity and its evolution with time during the first minutes of hydration is essential to prepare homogeneous specimens, which will have consequences on the final properties. No relevant differences in the phase assemblage of the pastes during time were found in the selected pastes to justify the differences in the mechanical strengths. Thus, processing is the key to obtain samples with very good mechanical performance. Finally, optimised ABY and dABY mortars showed mechanical strengths similar to PC at certain ages, but releasing ~13% less CO_2. The optimised ABY mortar showed compressive strengths of 71.6, 76.6, 86.9, 98.2 MPa at 7, 28, 56 and 180 days, respectively, and the values for the optimised dABY mortar were 40.7, 74.9, 81.9 and 83.3 MPa at the same ages, respectively. The optimised dBAY mortar showed an important increase in compressive strength from 7 to 28 days due to the higher content and reaction of belite polymorphs.

Acknowledgements

This work is part of the PhD of Mr. Jesus D. Zea-Garcia. This research has been supported by Spanish MINECO and FEDER [BIA2017-82391-R research project and I3 (IEDI-2016-0079) program].

Figure captions

Figure 1. SEM micrographs of the fracture surfaces of ABY (a) and dABY (b) die-pressed clinker pellets, and ABY (c) and dABY (d) clinker powders after milling.

Figure 2. Deflocculation curves at 50 s^{-1} (a) and 200 s^{-1} (b) of ABY and dABY as a function of SP content. Viscosity vs. w/c ratio of ABY (c) and dABY (d) pastes at different shear rates (50 s^{-1} solid lines and 200 s^{-1} dashed lines).

Figure 3. Evolution of the viscosity with time of ABY (a) and dABY (b) pastes, prepared with w/c=0.40 and 0.50, and 0.0, 0.4 and 1.0 wt% superplasticiser. Shear rate: 5 s^{-1}.

Figure 4. Compressive strength values of ABY (a) and dABY (b) mortars, prepared with w/c=0.40 and 0.50, and 0.4 and 1.0 wt% superplasticiser. Insets show photographs of selected cube (3 x 3 x 3 cm^3) mortars.

Figure 5. Phase assemblage as a function of time of ABY_0.40w/c_1.0wt%SP (a), ABY_0.50w/c_0.4wt%SP (b), dABY_0.40w/c_1.0wt%SP (c) and dABY_0.50w/c_0.4wt%SP (d). Dark solid blue stands form minor anhydrous phases while orange solid stands minor hydrated phases.

Figure 6. Ettringite phase evolution (a), ACn (b) free water evolution (c) of pastes prepared with w/c=0.40 and 1.0 wt% of SP and w/c=0.50 and 0.4 wt% of SP.

Table 1. Mineralogical composition (in weight percentage) determined by RQPA of both cements, including the ACn.

Table 2. Values of the thixotropic cycle of both family pastes prepared at different w/c ratios and different amounts of superplasticiser.

Table 3. Degree of reaction of the main phases (alite, belite and alpha-belite) at all studied ages for the four selected samples.

Table 1. Mineralogical composition determined by RQPA of both cements, including the ACn [8].

Phases	ABY (wt%)	dABY (wt%)
alite	25.9(3)	9.3(3)
β-belite	22.8(4)	26.3(4)
α'_H-belite	-	13.8(4)
ye'elimite	12.2(5)	5.5(2)
Brownmillerite[1]	3.4(2)	2.3(2)
Anhydrite[2]	13.5(5)	13.8(1)
Mayenite[3]	-	4.8(1)
CaO	0.5(1)	-
MgO	0.7(1)	-
F-ellestadite[4]	1.7(2)	1.9(2)
ACn	19(1)	22.2(7)
Total	100.0	100.0

[1] Brownmillerite: $Ca_4Al_2Fe_2O_{10}$, [2] Anhydrite: $CaSO_4$, [3] Mayenite: $Ca_{12}Al_{14}O_{33}$, [4] F-ellestadite: $Ca_{10(}SiO_4)_3(SO_4)_3F_2$

Table 2. Values of the thixotropic cycle of both family pastes prepared at different w/c ratios and different amounts of superplasticiser.

Cement paste	w/c	SP (wt%)	Thixotropic cycle (Pa/s)
ABY	0.40	0.0	5333
		0.1	7377
		0.2	3863
		0.3	4248
		0.4	2025
		0.5	3410
		1.0	813
	0.50	0.0	5201
		0.2	1522
		0.3	2503
		0.4	243
		1.0	227
	0.55	0.0	1000
		0.4	379
		1.0	148
dABY	0.40	0.0	4874
		0.1	6015
		0.2	6716
		0.3	5431
		0.4	5802
		0.5	7736
		0.7	7467
		1.0	1834
	0.50	0.0	2202
		0.4	625
		1.0	1597
	0.55	0.0	999

	0.4	154
	1.0	317

Table 3. Degree of reaction of the main phases (alite, belite and alpha-belite) at all studied ages for the four selected samples.

Age	ABY						d-ABY					
	0.40w/c, 1wt%SP			0.50w/c, 0.4wt%SP			0.40w/c, 1wt%SP			0.50w/c, 0.4wt%SP		
	alite	β-belite	α-belite	alite	β-belite	α-belite	alite	β-belite	α-belite	alite	β-belite	α-belite
1d	46	8	-	54	6	-	32	0	18	31	0	41
7d	69	4	-	77	14	-	67	0	13	73	0	25
28d	79	22	-	93	31	-	89	59	79	87	73	88
56d	92	41	-	91	63	-	92	70	89	79	81	89

REFERENCES

[1] I. Amato, Green cement: Concrete solutions, Nature. 494 (2013) 300–301. http://doi:10.1038/494300a.

[2] E. Gartner, H. Hirao, A review of alternative approaches to the reduction of CO_2 emissions associated with the manufacture of the binder in concrete, Cem. Concr. Res. 78 (2015) 126–142. https://doi.org/10.1016/j.cemconres.2015.04.012.

[3] T. Hanein, J.L. Galvez-Martos, M.N. Bannerman. Carbon footprint of calcium sulfoaluminate clinker production. J. Clean. Prod. 172 (2018) 2278-2287. https://doi.org/10.1016/j.jclepro.2017.11.183.

[4] N. Chitvoranund, B. Lothenbach, F. Winnefeld, C.W. Hargis, Synthesis and hydration of alite-calcium sulfoaluminate cement, Adv. Cem. Res. 29 (2016) 101-111. https://doi.org/10.1680/jadcr.16.00071.

[5] S. Ma, R. Snellings, X. Li, X. Shen, K.L. Scrivener, Alite-ye'elimite cement: Synthesis and mineralogical analysis, Cem. Concr. Res. 45 (2013) 15–20. https://doi:10.1016/j.cemconres.2012.10.020.

[6] R. Lili, L. Xiaocun, Q. Tao, L. Jian, Z. Deli, L. Yanjun, Influence of MnO_2 on the burnability and mineral formation of alite-sulphoaluminate cement clinker, Silic. Ind. 74 (2009) 183–188.

[7] D. Londono-Zuluaga, J.I. Tobon, M.A.G. Aranda, I. Santacruz, A.G. De La Torre, Clinkering and hydration of Belite-Alite-Ye´elimite cement, Cem. Concr. Compos. 80 (2017) 333–341. https://doi:10.1016/j.cemconcomp.2017.04.002.

[8] D. Zea-Garcia, M.A.G. Aranda, I. Santacruz, A.G. De la Torre, Alite-belite-ye'elimite cements: Effect of dopants on the clinker phase composition and properties, Cem. Concr. Res. 115 (2019) 192-202. https://doi.org/10.1016/j.cemconres.2018.10.019.

[9] G. Álvarez-Pinazo, I. Santacruz, L. León-Reina, M.A.G. Aranda, A.G. De la Torre, Hydration reactions and mechanical strength developments of iron-rich sulfobelite eco-cements, Ind. Eng. Chem. Res. 52 (2013) 16606–16614. https://doi:10.1021/ie402484e.

[10] M. Palacios, Y.F. Houst, P. Bowen, F. Puertas, Adsorption of superplasticizer admixtures on alkali-activated slag pastes, Cem. Concr. Res. 39 (2009) 670–677. https://doi.org/10.1016/j.cemconres.2009.05.005.

[11] A. Papo, L. Piani, Effect of various superplasticizers on the rheological properties of Porlant cement pastes, Cem. Concr. Res. 34 (2004) 2097-2101. https://doi.org/10.1016/j.cemconres.2004.03.017

[12] J. Björnstrom, S. Chandra, Effect of superplasticizers on the rheological properties of cements, Mat. Struct. 36 (2003) 685–692.

[13] F. Puertas, H. Santos, M. Palacios, S. Martínez-Ramírez, Polycarboxylate superplasticizer admixtures: effect on hydration, microstructure and rheological behaviour in cement pastes, Adv. Cem. Res. 17 (2005) 77–89. https://doi.org/10.1680/adcr.2005.17.2.77

[14] J. Gołaszewski, Influence of cement properties on new generation superplasticizers performance, Constr. Build. Mater. 35 (2012) 586-596. https://doi.org/10.1016/j.conbuildmat.2012.04.070.
[15] F. Ridi, L. Dei, E. Fratini, S.H. Chen, P. Baglioni, Hydration kinetics of tri-calcium silicate in the presence of superplasticizers, J. Phys. Chem. 107 (2003) 1056-1061. http://doi.org/10.1021/jp027346b.
[16] J. Rieger, J. Thieme, C. Schmidt, Study of precipitation reactions by X-ray microscopy: $CaCO_3$ precipitation and the effect of polycarboxylates, Langmuir 16 (2000) 8300-8305.
[17] W. Chang, H. Li, M. Wei, Z. Zhu, J. Zhang, M. Pei, Effects of polycarboxylic acid based superplasticiser on properties of sulphoaluminate cement, Mater. Res. Innovations 13 (2009) 7-10. https://doi.org/10.1179/143307509X402101.
[18] M. García-Maté, I. Santacruz, A.G. De la Torre, L. León-Reina, M.A.G. Aranda, Rheological and hydration characterization of calcium sulfoaluminate cement pastes, Cem. Concr. Comp., 34 (2012) 684–691. https://doi.org/10.1016/j.cemconcomp.2012.01.008.
[19] M. García-Maté, A.G. De la Torre, A. Cabeza, E.R. Losilla, M.A.G. Aranda, I. Santacruz, Tailored setting times with high compressive strengths in bassanite calcium sulfoaluminate eco-cements. Cem. Concr. Comp. 72 (2016) 39-47. https://doi.org/10.1016/j.cemconcomp.2016.05.021.
[20] A. Cuesta, J.D. Zea-Garcia, D. Londono-Zuluaga, A.G. De la Torre, I. Santacruz, O. Vallcorba, M. Dapiaggi, S.G. Sanfélix, M.A.G. Aranda, Multiscale understanding of tricalcium silicate hydration reactions, Sci. Rep. 8 (2018) 8544-8554. https://doi.org/10.1038/s41598-018-26943-y.
[21] J.D. Zea-Garcia, I. Santacruz, M.A.G. Aranda, A.G. De la Torre, Alite-belite-ye'elimite cements: Effect of dopants on the clinker phase composition and properties, Cem. Concr. Res. 115 (2019) 192-202.
[22] R.B. Von Dreele, A.C. Larson, General structure analysis system (GSAS), Los Alamos Natl. Lab. Rep. LAUR. 748 (2004) 86–748.
[23] P. Thompson, D.E. Cox, J.B. Hastings, Rietveld Refinement of Debye-Scherrer Synchrotron X-ray Data from A1203, J. Appl. Crystallogr. 20 (1987) 79–83. https://doi.org/10.1107/S0021889887087090.
[24] L.W. Finger, D.E. Cox, A.P. Jephcoat, Correction for powder diffraction peak asymmetry due to axial divergence, J. Appl. Crystallogr. 27 (1994) 892–900. https://doi.org/10.1107/S0021889894004218.
[25] Álvarez-Pinazo, A. Cuesta, M. García-Maté, I. Santacruz, E.R. Losilla, A.G. De la Torre, L. León-Reina, M.A.G. Aranda. Rietveld quantitative phase analysis of Yeelimite-containing cements. Cem. Concr. Res., 42 (2012) 960–971. https://doi.org/10.1016/j.cemconres.2012.03.018.
[26] R. Pérez-Bravo, G. Álvarez-Pinazo, J.M. Compana, I. Santacruz, E.R. Losilla, S. Bruque, A.G. De la Torre, Alite sulfoaluminate clinker: Rietveld mineralogical and SEM-EDX analysis, Adv. Cem. Res. 26 (2014) 10–20. https://doi.org/10.1680/adcr.12.00044

[27] D. Koumpouri, G.N. Angelopoulos, Effect of boron waste and boric acid addition on the production of low energy belite cement, Cem. Concr. Compos. 68 (2016) 1–8. https://doi.org/10.1016/j.cemconcomp.2015.12.009.
[28] G. Álvarez-Pinazo, I. Santacruz, M.A.G. Aranda MAG, A.G. De la Torre, Hydration of belite–ye'elimite–ferrite cements with different calcium sulfate sources, Adv. Cem. Res. 28 (2016) 529-543. https://doi.org/10.1680/jadcr.16.00030
[29] F. Bullerjahn, M. Zajac, M. Ben Haha, K.L. Scrivener, Factors influencing the hydration kinetics of ye'elimite; effect of mayenite, Cem. Concr. Res. 116 (2019) 113–119. doi:10.1016/J.CEMCONRES.2018.10.026.
[30] M.J. Sánchez-Herrero, A. Fernández-Jiménez, A. Palomo, $C_4A_3\underline{S}$ hydration in different alkaline media, Cem. Concr. Res. 46 (2013) 41-49. https://doi.org/10.1016/j.cemconres.2013.01.008.

ABY

dABY

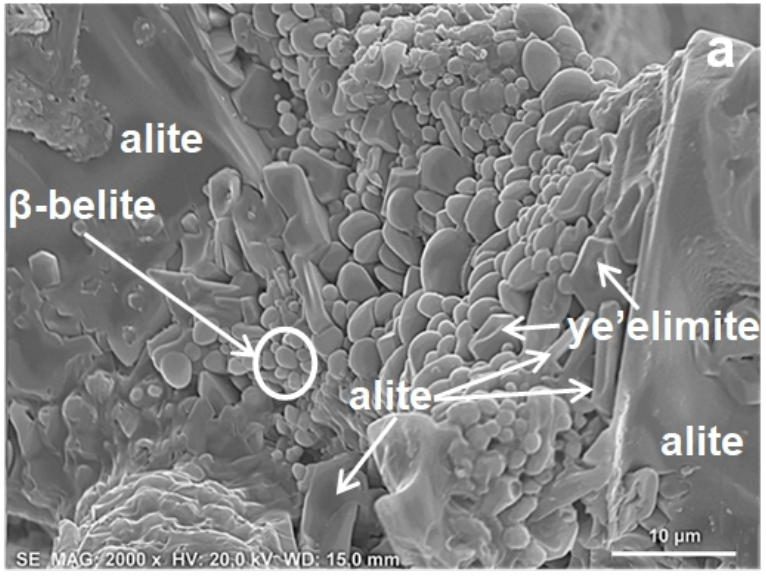
a
alite
β-belite
ye'elimite
alite
alite
10 µm
SE MAG: 2000 x HV: 20.0 kV WD: 15.0 mm

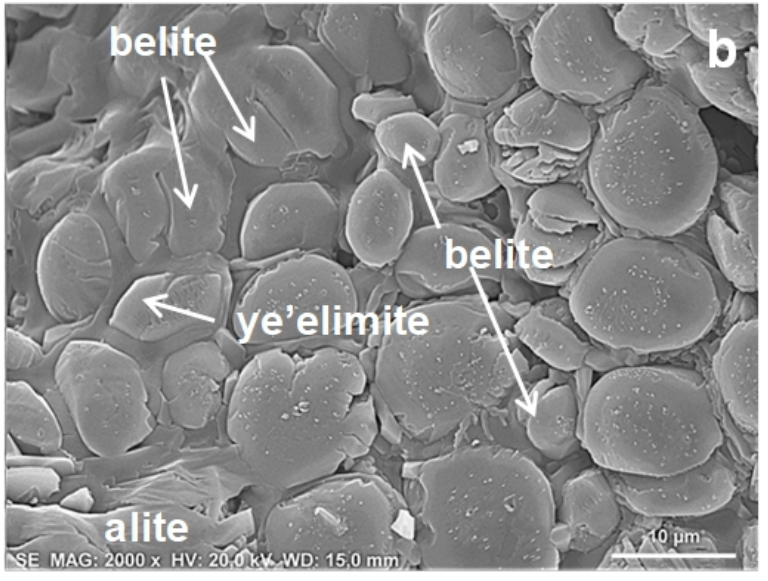
b
belite
belite
ye'elimite
alite
10 µm
SE MAG: 2000 x HV: 20.0 kV WD: 15.0 mm

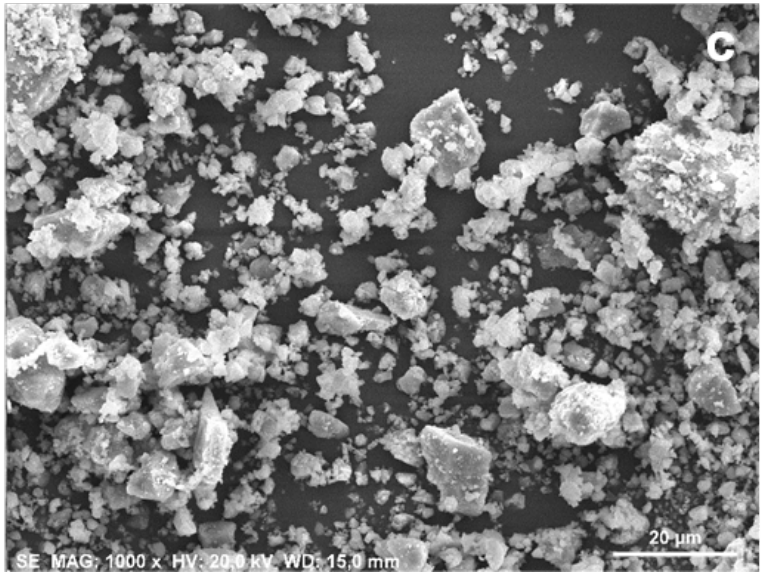
c
20 µm
SE MAG: 1000 x HV: 20.0 kV WD: 15.0 mm

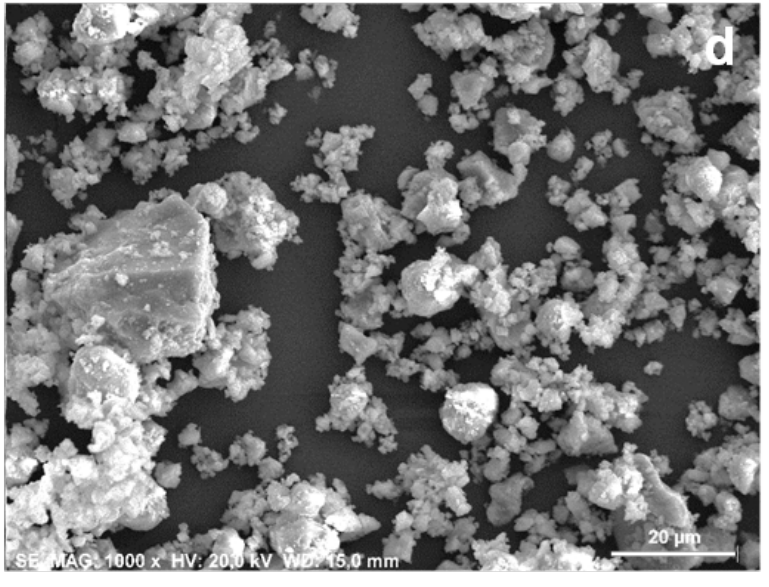
d
20 µm
SE MAG: 1000 x HV: 20.0 kV WD: 15.0 mm

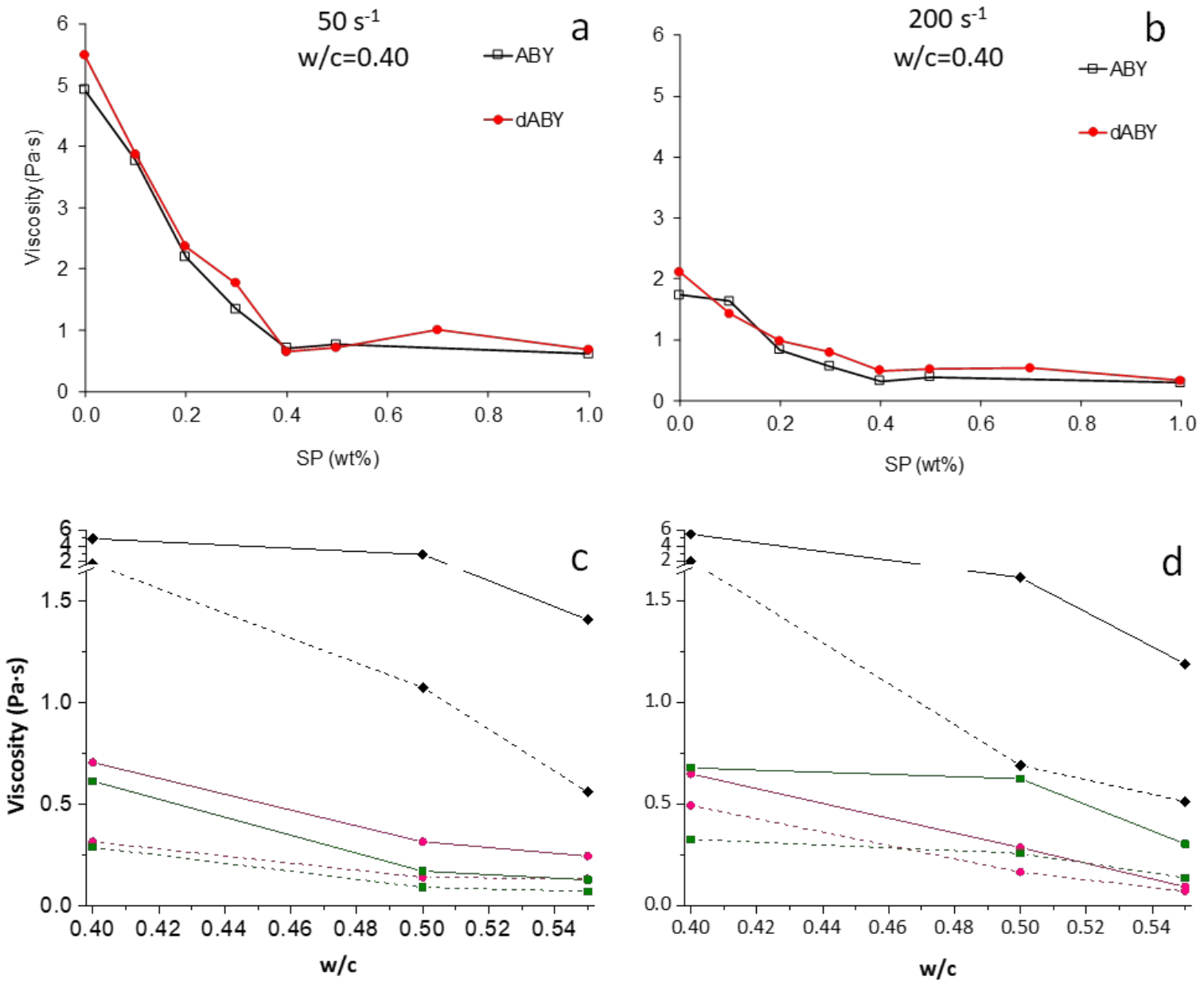
50 s-1
w/c=0.40
a
ABY
dABY
Viscosity (Pa·s)
SP (wt%)
200 s-1
w/c=0.40
b
ABY
dABY
SP (wt%)
c
Viscosity (Pa·s)
w/c
d
w/c

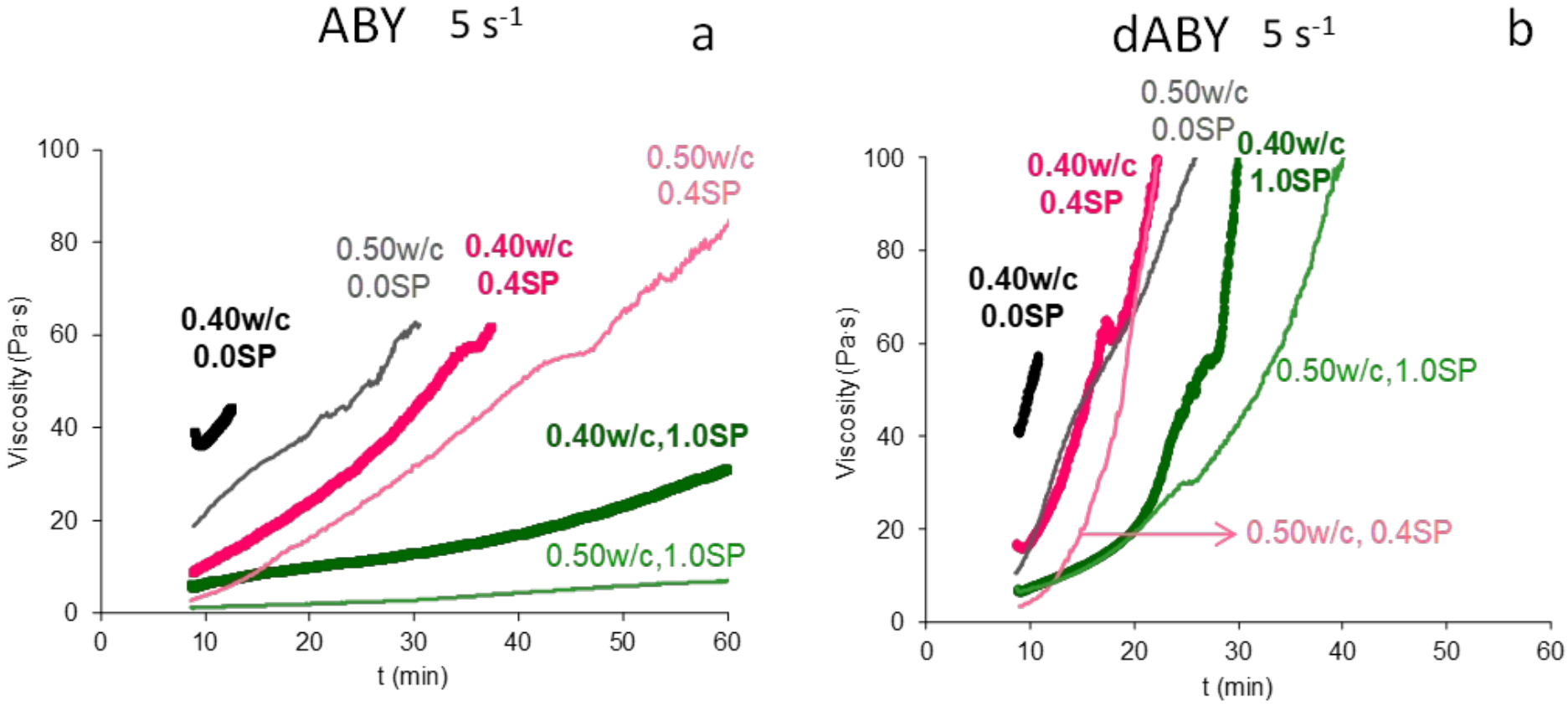
ABY 5 s-1
a
Viscosity (Pa·s)
t (min)
0.40w/c 0.0SP
0.50w/c 0.0SP
0.40w/c 0.4SP
0.50w/c 0.4SP
0.40w/c,1.0SP
0.50w/c,1.0SP
dABY 5 s-1
b
0.50w/c 0.0SP
0.40w/c 0.4SP
0.40w/c 1.0SP
0.40w/c 0.0SP
0.50w/c,1.0SP
0.50w/c, 0.4SP

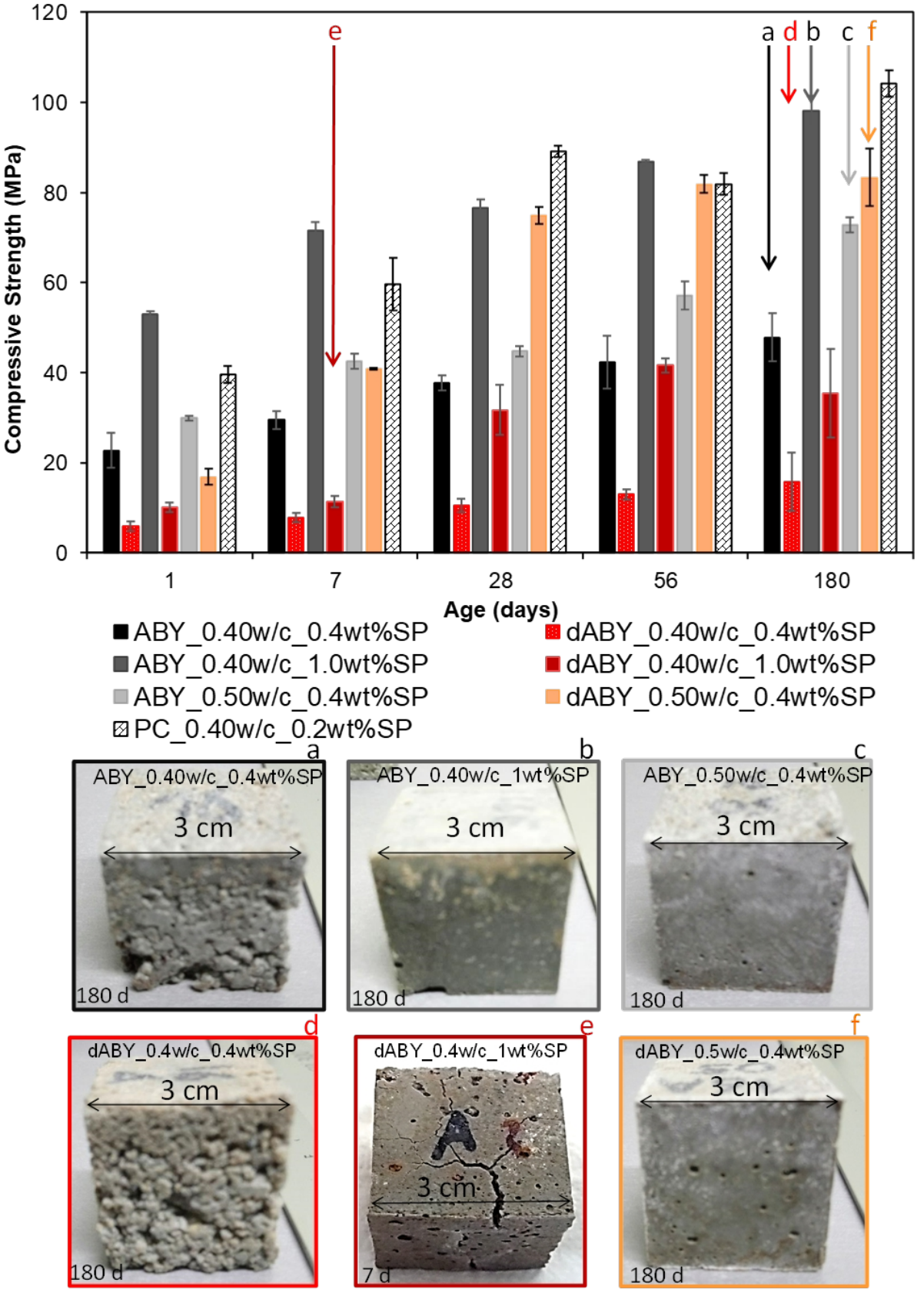
Compressive Strength (MPa)
120
100
80
60
40
20
0
1
7
28
56
180
Age (days)
a
d
b
c
f
e
ABY_0.40w/c_0.4wt%SP
ABY_0.40w/c_1.0wt%SP
ABY_0.50w/c_0.4wt%SP
PC_0.40w/c_0.2wt%SP
dABY_0.40w/c_0.4wt%SP
dABY_0.40w/c_1.0wt%SP
dABY_0.50w/c_0.4wt%SP
a
ABY_0.40w/c_0.4wt%SP
3 cm
180 d
b
ABY_0.40w/c_1wt%SP
3 cm
180 d
c
ABY_0.50w/c_0.4wt%SP
3 cm
180 d
d
dABY_0.4w/c_0.4wt%SP
3 cm
180 d
e
dABY_0.4w/c_1wt%SP
3 cm
7 d
f
dABY_0.5w/c_0.4wt%SP
3 cm
180 d

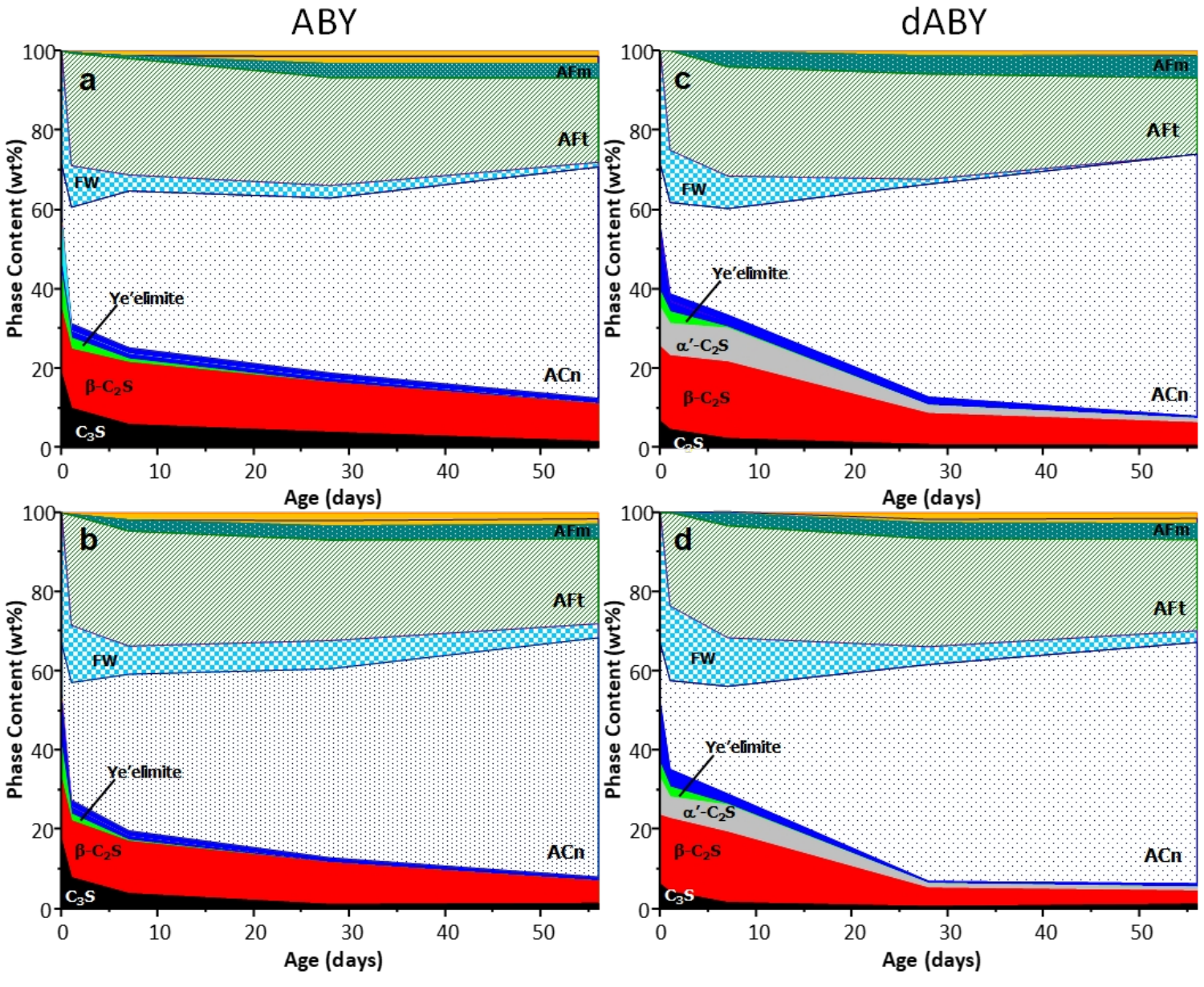
ABY
dABY
a
b
c
d
AFm
AFt
FW
Ye'elimite
α'-C2S
β-C2S
C3S
ACn
Phase Content (wt%)
Age (days)
0
20
40
60
80
100
0
10
20
30
40
50

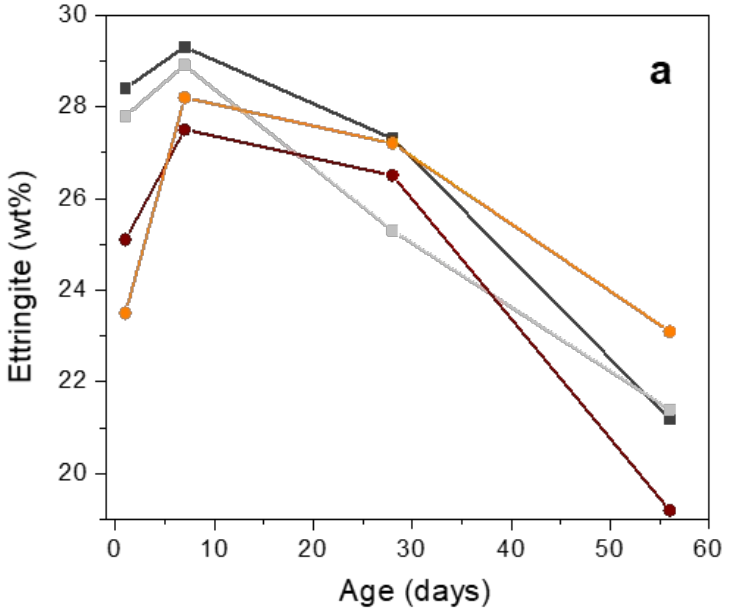
a
Ettringite (wt%)
Age (days)

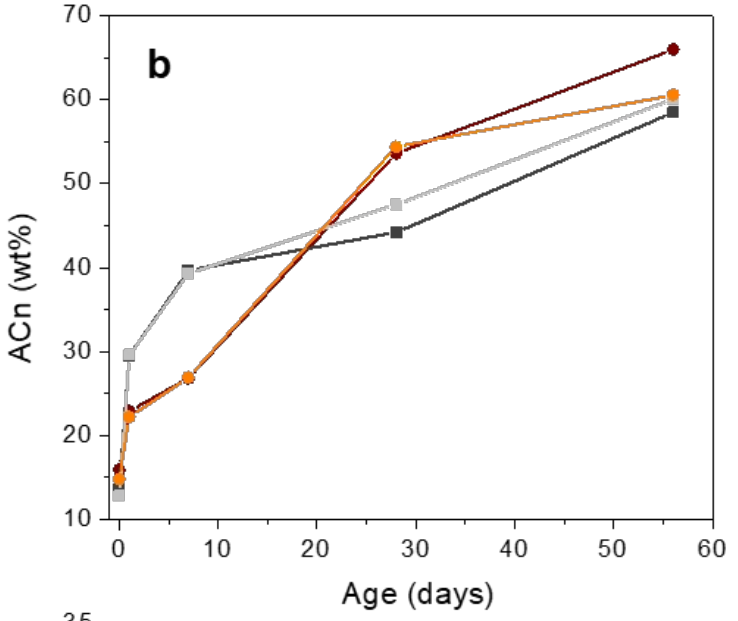
b
ACn (wt%)
Age (days)

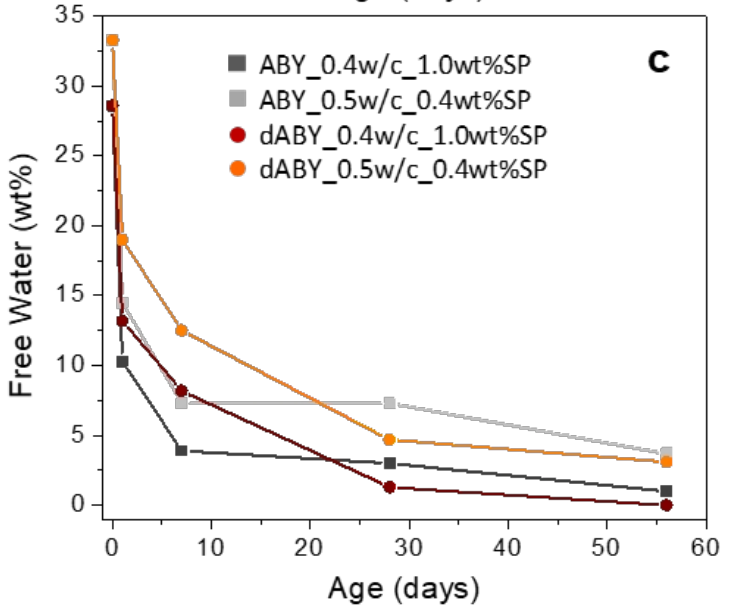
c
ABY_0.4w/c_1.0wt%SP
ABY_0.5w/c_0.4wt%SP
dABY_0.4w/c_1.0wt%SP
dABY_0.5w/c_0.4wt%SP
Free Water (wt%)
Age (days)

Dr. Isabel Santacruz Cruz
Departamento de Química Inorgánica
Facultad de Ciencias
Universidad de Málaga
29071 - MALAGA, Spain
Int- 34-952131878, Fax.: Int- 34-952131870

Málaga, 23th September 2019

In order to fulfill the revision of our article entitled “Processing and characterisation of standard and doped alite-belite-ye’elimite ecocement pastes and mortars” with reference CEMCON_2019_639.

The authors declare that they have no conflict of interest.

Yours Sincerely,

Isabel Santacruz

Supplementary Information

Processing and characterisation of standard and doped alite-belite-ye'elimite cement pastes and mortars

Jesus D. Zea-Garcia[a], Angeles G. De la Torre[a], Miguel A.G. Aranda[a,b], Isabel Santacruz[a*]

[a] Departamento de Química Inorgánica, Cristalografía y Mineralogía, Universidad de Málaga, Málaga, 29071, Spain.

[b] ALBA Synchroton, Carrer de la Lum, 2-26, Cerdanyola, 08290, Barcelona-Spain.

* email: isantacruz@uma.es. Phone: +34.952131878. Fax: +34.952131870

Figure S1. Flow curves of ABY (left) and dABY (right) pastes prepared at w/c=0.40 and different superplasticiser (SP) contents. Pastes prepared at w/c=0.50 with 0.4 wt% SP are also shown for the sake of comparison.

Figure S2. Rietveld plots of the optimised ABY (w/c=0.40, 1.0 wt% SP) (a), and dABY (w/c=0.50, 0.4 wt% SP) (b) pastes, at 56 hydration days.

Table S1. Phase assemblage of selected ABY and dABY pastes at 0 hydration days.

Table S2. Phase assemblage of selected ABY and dABY pastes at 1 hydration day.

Table S3. Phase assemblage of selected ABY and dABY pastes at 7 hydration days.

Table S4. Phase assemblage of selected ABY and dABY pastes at 28 hydration days.

Table S5. Phase assemblage of selected ABY and dABY pastes at 56 hydration days.

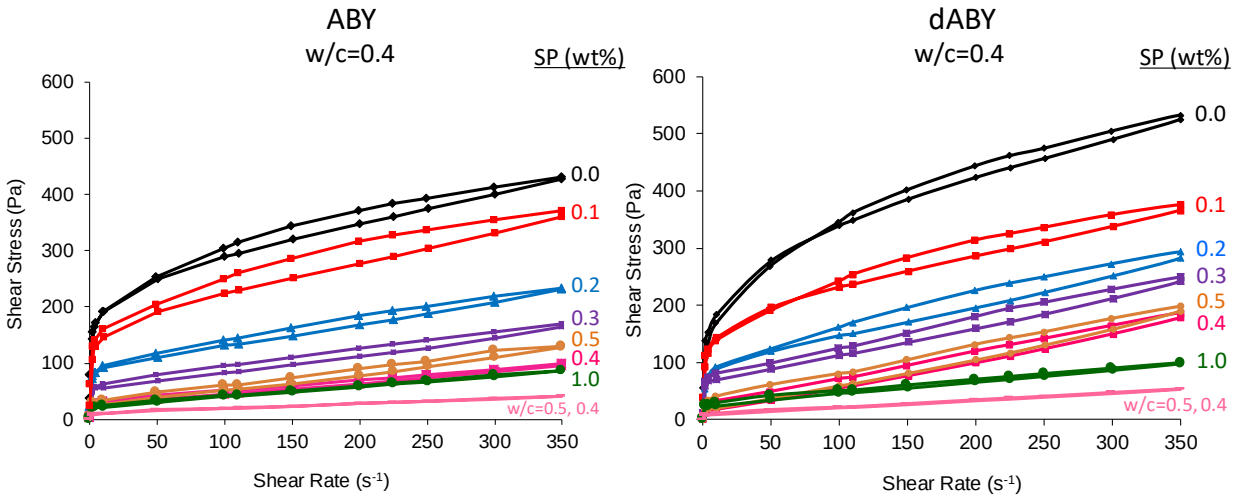

Figure S1. Flow curves of ABY (left) and dABY (right) pastes prepared at w/c=0.40 and different superplasticiser (SP) contents. Pastes prepared at w/c=0.50 with 0.4 wt% SP are also shown for the sake of comparison.

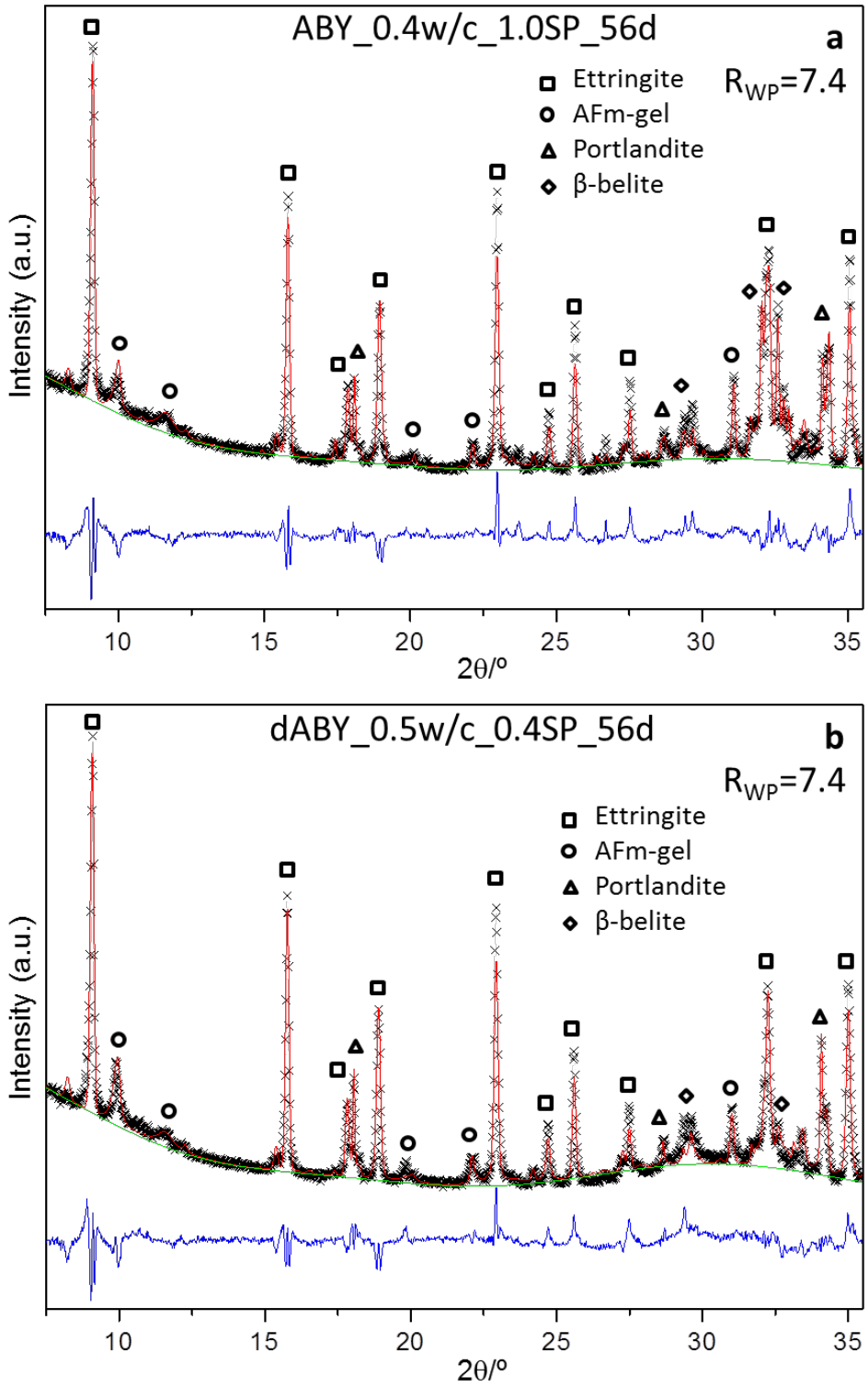

Figure S2. Rietveld plots of the optimised ABY (w/c=0.40, 1.0 wt% SP) (a), and dABY (w/c=0.50, 0.4 wt% SP) (b) pastes, at 56 hydration days.

Table S1. Phase assemblage of selected ABY and dABY pastes at 0 hydration days.

Phases	ABY		d-ABY	
	0.40w/c 1wt%SP	**0.50w/c 0.4wt%SP**	**0.40w/c 1wt%SP**	**0.50w/c 0.4wt%SP**
Alite	18.5(3)	17.3(3)	6.6(3)	6.2(3)
β-belite	16.2(4)	15.2(4)	18.8(4)	17.5(4)
α'_H- belite	-	-	9.9(4)	9.2(4)
ye'elimite	8.7(5)	8.2(5)	4.0(2)	3.8(2)
Brownmillerite[1]	2.4(2)	2.3(2)	1.7(2)	1.6(2)
Anhydrite[2]	9.7(5)	9.0(5)	9.8(1)	9.2(1)
Mayenite[3]	-	-	3.4(1)	3.2(1)
CaO	0.5(1)	0.4(1)	-	-
MgO	0.6(1)	0.5(1)	-	-
F-ellestadite[4]	1.2(2)	1.1(2)	1.3(2)	1.3(2)
ACn	**13.7(1)**	**12.8(1)**	**15.9(7)**	**14.8(7)**
H_2O-FW	**28.6**	**33.3**	**28.6**	**33.3**
Total	100.1	100.1	100.0	100.1

[1] Brownmillerite: $Ca_4Al_2Fe_2O_{10}$, [2] Anhydrite: $CaSO_4$, [3] Mayenite: $Ca_{12}Al_{14}O_{33}$, [4] F-ellestadite: $Ca_{10}(SiO_4)_3(SO_4)_3F_2$

Table S2. Phase assemblage of selected ABY and dABY pastes at 1 hydration day.

Phases	ABY		d-ABY	
	0.40w/c 1wt%SP	**0.50w/c 0.4wt%SP**	**0.40w/c 1wt%SP**	**0.50w/c 0.4wt%SP**
Alite	9.9(2)	8.0(2)	4.5(2)	4.3(1)
β-belite	14.9(3)	14.3(3)	18.6(3)	18.6(3)
α'_H- belite	-	-	8.1(3)	5.4(1)
ye'elimite	2.8(2)	1.7(2)	3.0(1)	2.6(1)
Brownmillerite[1]	1.7(1)	1.7(1)	1.6(1)	1.6(1)
Mayenite[3]	-	-	1.2(1)	1.2(1)
F-ellestadite[4]	1.9(2)	1.8(1)	1.8(1)	1.6(1)
Ettringite[5]	**28.4(2)**	**27.8(2)**	**25.1(2)**	**23.5(2)**
AFm-gel[6]	0.19(8)	0.17(9)	-	-
Portlandite[8]	0.44(4)	0.41(4)	-	-
ACn	**29.5(5)**	**29.6(5)**	**22.9(5)**	**22.2(4)**
H_2O-FW	**10.3**	**14.5**	**13.2**	**19.0**
Total	100.0	100.0	100.0	100.0

[1] Brownmillerite: $Ca_4Al_2Fe_2O_{10}$, [3] Mayenite: $Ca_{12}Al_{14}O_{33}$, [4] F-ellestadite: $Ca_{10(}SiO_4)_3(SO_4)_3F_2$, [5] Ettringite: $Ca_6Al_2(SO_4)_3(OH)_{12}\cdot 26H_2O$, [6] AFm-gel: $Ca_4Al_2(SO_4)(OH)_{12}\cdot 6H_2O$, [8] Portlandite: $Ca(OH)_2$

Table S3. Phase assemblage of selected ABY and dABY pastes at 7 hydration days.

Phases	ABY		d-ABY	
	0.40w/c 1wt%SP	**0.50w/c 0.4wt%SP**	**0.40w/c 1wt%SP**	**0.50w/c 0.4wt%SP**
alite	5.8(2)	4.0(3)	2.2(2)	1.7(2)
β-belite	15.6(3)	13.0(3)	19.3(3)	17.7(3)
α'_H- belite	-	-	8.6(3)	6.9(2)
ye'elimite	0.9(1)	0.4(1)	0.33(4)	0.18(5)
Brownmillerite[1]	1.2(1)	0.9(1)	1.1(1)	0.9(1)
F-ellestadite[4]	1.6(1)	1.5(1)	1.9(1)	1.7(1)
Ettringite[5]	**29.3(2)**	**28.9(2)**	**27.5(2)**	**28.2(2)**
AFm-gel[6]	0.8(1)	2.9(1)	4.0(2)	3.2(3)
Portlandite[8]	1.2(1)	1.9(1)	0.16(4)	0.22(4)
ACn	**39.7(5)**	**39.3(5)**	**26.8(5)**	**26.9(5)**
H_2O-FW	**3.9**	**7.3**	**8.2**	**12.5**
Total	100.0	100.1	100.1	100.1

[1] Brownmillerite: $Ca_4Al_2Fe_2O_{10}$, [4] F-ellestadite: $Ca_{10(}SiO_4)_3(SO_4)_3F_2$, [5] Ettringite: $Ca_6Al_2(SO_4)_3(OH)_{12}\cdot 26H_2O$, [6] AFm-gel: $Ca_4Al_2(SO_4)(OH)_{12}\cdot 6H_2O$, [8] Portlandite: $Ca(OH)_2$

Table S4. Phase assemblage of selected ABY and dABY pastes at 28 hydration days.

Phases	ABY		d-ABY	
	0.40w/c 1wt%SP	**0.50w/c 0.4wt%SP**	**0.40w/c 1wt%SP**	**0.50w/c 0.4wt%SP**
alite	3.8(2)	1.2(1)	0.7(2)	0.7(1)
β-belite	12.6(3)	10.5(2)	7.8(2)	4.7(1)
α'_H- belite	-	-	2.1(2)	1.1(1)
Brownmillerite[1]	0.9(2)	-	0.6(1)	-
F-ellestadite[4]	1.5(1)	1.3(1)	1.5(1)	0.6(1)
Ettringite[5]	**27.3(2)**	**25.3(2)**	**26.5(2)**	**27.2(2)**
AFm-gel[6]	3.5(1)	3.6(2)	4.7(2)	4.0(2)
Katoite[7]	1.8(1)	1.3(1)	-	0.8(1)
Portlandite[8]	1.5(1)	2.0(1)	1.2(1)	1.9(1)
ACn	**44.2(5)**	**47.5 (4)**	**53.6(5)**	**54.4(3)**
H_2O-FW	**3.0**	**7.3**	**1.3**	**4.7**
Total	100.1	100.0	100.0	100.1

[1] Brownmillerite: $Ca_4Al_2Fe_2O_{10}$, [4] F-ellestadite: $Ca_{10}(SiO_4)_3(SO_4)_3F_2$, [5] Ettringite: $Ca_6Al_2(SO_4)_3(OH)_{12}\cdot 26H_2O$, [6] AFm-gel: $Ca_4Al_2(SO_4)(OH)_{12}\cdot 6H_2O$, [7] Katoite: $Ca_3Al_2SiO_8\cdot 4H_2O$, [8] Portlandite: $Ca(OH)_2$

Table S5. Phase assemblage of selected ABY and dABY pastes at 56 hydration days.

Phases	ABY		d-ABY	
	0.40w/c 1wt%SP	**0.50w/c 0.4wt%SP**	**0.40w/c 1wt%SP**	**0.50w/c 0.4wt%SP**
alite	1.5(1)	1.5(1)	0.5(1)	1.3(1)
β-belite	9.5(2)	5.6(2)	5.7(2)	3.3(2)
α'_H-belite	-	-	1.1(1)	1.0(1)
F-ellestadite[4]	1.4(1)	1.1(1)	0.6(1)	0.9(1)
Ettringite[5]	**21.2(2)**	**21.4(2)**	**19.2(2)**	**23.1(2)**
AFm-gel[6]	3.8(1)	3.7(2)	5.5(2)	4.0(1)
Katoite[7]	1.7(1)	1.4(1)	0.5(1)	1.1(1)
Portlandite[8]	1.5(1)	1.5(1)	0.9(1)	1.6(1)
ACn	**58.5(4)**	**60.1(4)**	**66.0(4)**	**60.6(4)**
H_2O-FW	**1.0**	**3.7**	**0.0**	**3.1**
Total	100.1	100.0	100.0	100.0

[4] F-ellestadite: $Ca_{10}(SiO_4)_3(SO_4)_3F_2$, [5] Ettringite: $Ca_6Al_2(SO_4)_3(OH)_{12}\cdot 26H_2O$, [6] AFm-gel: $Ca_4Al_2(SO_4)(OH)_{12}\cdot 6H_2O$, [7] Katoite: $Ca_3Al_2SiO_8\cdot 4H_2O$, [8] Portlandite: $Ca(OH)_2$